ORIGINAL ARTICLE

Space-resolved quantitative mechanical measurements of soft and supersoft materials by atomic force microscopy

Massimiliano Galluzzi[1,2], Chandra S Biswas[1,2], Yuhang Wu[1], Qiao Wang[1], Bing Du[1] and Florian J Stadler[1]

Atomic force microscopy (AFM) has proven to be a valuable instrument to characterize quantitatively the mechanical and morphological properties of soft materials. For medium and hard samples ($E > 1$ MPa), the nanomechanical accuracy of AFM is well established and ascertained. However, for soft samples, the experimental setup and data analysis for AFM are not yet firmly established. A calibration obtained for homogeneous samples with a Young's modulus ranging from 100 Pa to a few kPa will prove its usefulness for nanomechanical AFM investigations of soft biological specimens, such as living cells and extracellular matrices. For this purpose, poly(N-isopropylacrylamide) (PNIPAM) hydrogels were synthesized in different methanol–water mixtures to produce a series of homogeneous samples with finely tunable mechanical properties. These samples allowed the comparison and validation of AFM force spectroscopy results using macroscopic and rheological techniques. In AFM measurements, the geometry of the indenter is fundamental to the model used for data interpretation; therefore, experiments were carried out using spherical micrometric and standard pyramidal sharp probes. Moreover, a PNIPAM gel embedded with hard microspheres was analyzed, which showed the capability of AFM for measuring the local mechanical properties of heterogeneous samples.

INTRODUCTION

Atomic force microscope (AFM) has great potential as a tool for the quantitative characterization of mechanical properties of soft materials[1,2] (including biological specimens[3–10]) with high spatial resolution. By controlling the force and application point at the nanoscale, mechanical measurements can be coupled with topographical information, which opens up the possibility of investigating heterogeneous samples. The AFM force spectroscopy technique is well established and widely used for medium/hard samples ($E > 1$ MPa). However, only a few studies have focused on materials with a Young's modulus in the range between 0.1 and 10 kPa, which mostly includes soft biological materials with high complexity.[9,10] Hence, because of the heterogeneity of these materials, it was not possible to determine whether the obtained moduli were accurate. For this purpose, a recently developed technique, PeakForce quantitative nanomechanical mapping, has enabled a simultaneous quantitative nanomechanical investigation with imaging at high resolution and high speed. PeakForce quantitative nanomechanical mapping is extremely difficult for soft samples ($E < 100$ kPa) in liquid because of dragging forces, increased noise and a poorly defined contact with the samples. Therefore, AFM force spectroscopy of soft materials is currently being investigated and overcoming the lower stiffness limit of samples remains a technical challenge.

As discussed previously,[8] the experimental setup and data analysis required for the nanomechanical investigation of soft samples using AFM are complex, and subtle problems can arise, which compromise the ability to produce quantitative results. The most critical experimental parameters are the geometry of the probe, the elastic constant of the cantilever, the determination of the contact point between tip and sample and the validity of the contact mechanic model that describes the indentation process. Herein, we will present a discussion about these critical parameters; in particular, we underline the advantages and disadvantages of using sharp pyramidal probes and spherical colloidal probes. Colloidal probes possess a micrometric radius that results in superior performance and stability during mechanical measurements but sacrifices part of the capability for spatial resolution. For soft samples (especially biological ones), colloidal probes represent a good solution because of reduced local pressure and a less sharp curvature (to prevent damage to the sample and guarantee the validity of linear elastic models), well-defined

2

geometry and capability for mesoscopically averaged mechanical characterization. Sharp probes, due to their nanometric apex, represent the best choice for nanomechanical analysis if high local pressure is required to cause significant indentation (stiff samples) or if nanometric lateral resolution must be achieved. Both types of tips were used on the same samples in this work to provide a complete validation for future applications.

To test and characterize the geometric differences, a series of soft and supersoft poly(N-isopropylacrylamide) (PNIPAM) hydrogels were produced by varying the solvent (water–methanol mixture) composition during synthesis.[11,12] In this way, the internal structure of the hydrogel undergoes a structural modification, which results in greatly tunable mechanical properties of the hydrogels (from the 100 Pa to 10 kPa range). The mechanical properties of these gels are frequency-independent in the accessible range, homogeneous and linear; the gels represent a good model material to compare quantitatively and validate AFM results with macroscopic mechanical measurements obtained using a rheometer. This calibration will be very useful for relevant biological applications; in addition, the Young's modulus range under investigation is important for soft biomaterials, such as living cells, soft tissues and extracellular matrices.[8–10,13]

For soft and supersoft samples, a rheometer has numerous advantages compared with AFM: it provides access to the complete mechanical properties of the whole sample in either the shear mode or compression mode, it enables the measurement of the frequency-dependent viscoelasticity for liquids and supersoft materials ($E < 100$ Pa), and it exhibits good temperature control. However, AFM possesses the unique advantage that mechanical properties can be spatially resolved depending on the probe geometry and indentation depth, whereas a rheometer measurement is limited to averaged properties of the whole sample.

To highlight the spatial resolution obtained using AFM, a composite of the PNIPAM-based hydrogel was prepared in water by suspending aluminum oxide (Al_2O_3) nanoparticle aggregates during the synthesis; in addition, nanoparticle fillers were used to improve the mechanical stability of soft polymers and hydrogels and possibly to fine-tune their properties.[14,15] Hard particles within the soft gel matrix form a randomly heterogeneous nanocomposite sample, which is ideal for testing space-resolved mechanical properties.

MATERIALS AND METHODS

The preparation of hydrogel samples is accurately described in the Supplementary Information (SI.1 Chemicals, SI.2 gels synthesis and Supplementary Table 1 about chemical synthesis). The details of the experimental techniques used for scanning electron microscopy (SEM) and rheological tests are described in SI.3 and SI.4, respectively. Example of shear modulus measurements by rheometer is presented in Supplementary Figure 4, while experimental values are shown in Supplementary Table 2.

AFM mechanical properties

The local elasticity of the PNIPAM gels and calibrated PDMS (poly-dimethylsiloxane) samples were probed with a commercial AFM Dimension Icon (Bruker, Santa Barbara, CA, USA) in the force volume (FV) mechanical imaging mode.[1] In an FV experiment, a force curve (FC) is obtained by vertically indenting the AFM tip at every point of a regular matrix in the selected area, which yields the local mechanical response at every point probed. The morphology is reconstructed from the ensemble of the recorded FC, thereby producing a 1:1 correspondence between the morphology and the map of the mechanical properties.

Depending on the mechanical properties of the sample, the ramp length (the total length related to the movement of the tip outside the sample plus the

indentation depth into the sample) was varied between $L = 5$ and 10 µm and a maximum force $F \approx 5$ nN for ultrasoft hydrogels and $F \approx 30$ nN for hard hydrogels was applied while the tip indentation velocity was maintained at $v \approx 20$ µm s^{-1}. The resolutions used for imaging and to obtain the FCs are indicated in the results and discussion of each measurement. For each sample and condition, a series of 10–12 FV measurements (64×64 resolution) were performed in different macroscopic positions to improve the statistical reliability of the experiments. All samples were imaged while they were immersed in deionized water at room temperature ($T = 23$ °C).

Probes with different geometries were used: sharp pyramidal commercial probes (MLCT from Bruker) with a cone semiangle of 17°, cantilevers with an elastic constant $k \approx 0.08$ N m^{-1} (for PDMS calibration samples, a tip with $k \approx 40$ N m^{-1} was used) and spherical colloidal probes (NovaScan, Ames, IA, USA) with a radius of 2550 nm and a nominal k of 0.06 N m^{-1}. The exact geometry of every tip used in the experiments was analyzed by scanning electron microscopy. Moreover, geometry and status of spherical colloidal probes were additionally confirmed by reverse AFM imaging on calibration standard TGT1, as shown in Supplementary Figure 5. The elastic spring constant was calibrated for each tip in air using the thermal tune method.[16]

Data analysis

Young's moduli were evaluated by data analysis performed in a Matlab (MathWorks, Natick, MA, USA) environment. A real-time graphic user interface analysis was developed by simplifying the accepted custom-built routine for nanomechanical properties of living cells.[8,17,18] Finite thickness correction is unnecessary because of the thickness of macroscopic samples.[13] Raw AFM data were preprocessed to obtain FCs (F (nN)) vs indentation (δ (nm)).[1] The crucial part during preprocessing is determining the contact point between the tip and the surface, which represents the origin of the indentation axis. In particular, in a liquid environment, the absence of adhesive interactions and the increased level of noise prevent the use of standard contact point recognition methods. A histogram of the force axis is produced for each FC, and the non-contact part is observed as a sharply defined Gaussian distribution (see Supplementary Figure 2 as an example). The region of the FC above the width of the Gaussian distribution is considered as the indentation for the fitting procedure. The total indentation length is used for topography correction; specifically, the direct output from the FV height map is related to the maximum indentation, which results in a compressed morphology. The indentation map must be added to the compressed morphology to obtain the best estimation of the sample surface at zero force. This correction is of paramount importance for heterogeneous samples where the indentation is influenced by the local Young's modulus.

After pretreatment, the indentation curves are fitted using the Hertz model (1) if spherical probes are used, or the Sneddon model (with the Bilodeau approximation for four-sided pyramids instead of a conical indenter) (2) for sharp probes:[19,20]

$$F = \frac{4}{3} \frac{E\sqrt{R}}{(1 - \nu^2)} \delta^{3/2} \quad \text{(Hertz)} \tag{1}$$

$$F = 0.7453 \frac{E \tan \alpha}{(1 - \nu^2)} \delta^2 \quad \text{(Sneddon)} \tag{2}$$

where E, ν, R and α represent the local Young's modulus, the Poisson ratio (0.5), the radius of the colloidal probe and the averaged half-opening angle of the four-sided pyramidal indenter, respectively.

The models used here were developed assuming a linear relationship between stress and strain, and, in particular, the Hertz model has an additional constraint of small deformation and a large tip radius ($\delta/R \ll 1$). In comparison with biological samples,[8,13] hydrogels represent a good candidate for these models because they are homogeneous, isotropic and linearly elastic, and they can be considered a half-infinite space that is subjected to small strain. With the sample totally immersed in solution, the adhesion between the tip and sample is small and negligible compared with the elastic force. A complete FC with approaching and retracting parts, for the series of hydrogels studied, is shown in Supplementary Figure 1. Therefore, despite its severe constraints and simplicity, the Hertz model represents a good approximation and is also the

best starting point to develop corrections for finite thickness and multilayered structures.[13] Moreover, the possibility of controlling the indentation range during the fitting procedure is fundamental for not exceeding the model limits.

As discussed previously,[8] the accuracy of the Young's modulus values depends mostly on the accuracy of the cantilever elastic constant k (relative error $\approx 10\%$), the probe geometry (with a negligible relative error for colloidal tips but a 10–15% relative error for sharp tips) and the determination of the contact point (a 10–20 nm error). The error related to calibration of these experimental parameters is evaluated using the Lybanon method,[21] which is based on Monte Carlo simulations (see Puricelli *et al*.[8] for a detailed discussion). For a single FV measurement, the error associated must take this calibration error and the variability of Young's moduli in the FV area, that is, the width of log normally distributed values, into account. The final error characteristics depend on the error of a single FV and its variation due to measurements in different macroscopic locations on the same sample.

Calibration

To test the experimental setup in a liquid environment and to validate the developed analysis protocol using the Matlab graphic user interface, a set of mechanical calibration samples supplied from Bruker were measured. These samples, standard thick films of PDMS polymer with calibrated Young's moduli, were provided for PeakForce quantitative nanomechanical mapping calibration and therefore represent easy samples for FV characterization (the mechanical map for the 3.5 and 2.5 MPa samples are shown in Figures 1a and b, respectively). A standard pyramidal probe (semiangle $\theta = 17°$ and $k = 39\,\text{N m}^{-1}$) was used in aqueous environment. Data analysis using the Sneddon model (with the Bilodeau correction) results in 3.48 ± 0.06 and 2.37 ± 0.06 MPa (Figure 1c) for the correctness of the FV measurements and the evaluation method for rubbery samples, respectively. For both samples, examples of the raw FC with the Bilodeau–Sneddon fit are shown in Figure 1d.

Although these results, 3.48 ± 0.06 and 2.37 ± 0.06 MPa, are in good agreement with calibrated values of 3.5 and 2.5 MPa, Young's moduli of the studied hydrogels are supposed to be 3–4 orders of magnitude lower and, hence, shear modulus measurements have to be used as the benchmark.

RESULTS AND DISCUSSION

From the SEM images in Figure 2, it is clear that the gel synthesized in pure water (hydrogel-1) is nonporous (Figure 2a), as indicated by the absence of any visible pores. This is mainly due to the high homogeneity of the solvent system for the PNIPAM chain, in which the polymer network presents a coiled conformation.[17,18] The gel synthesized in the presence of the 1:3 water–methanol mixture ($v\,v^{-1}$) (hydrogel-2) is slightly porous as very few pores are visible (Figure 2b). This is because the gel synthesized outside of the cononsolvency region and solvent remained homogeneous for the PNIPAM chain segment throughout the synthesis. The gel synthesized in 1:1 water–methanol mixture ($v\,v^{-1}$) (hydrogel-3) shows a highly porous morphology, as is evident from Figure 2c. This is mainly due to the cononsolvency of the solvent mixture for the PNIPAM chain segment.[11] As a result, polymerization occurs in the heterogeneous phase, and, furthermore, the decomposition of the APS initiator is also significantly faster in the water–methanol mixture. Consequently, a highly porous gel was formed.[17,18] It is clear that only a variation in the compositions of the synthesis solvent results in significant changes to the gel morphology and mechanical properties.

Obtaining accurate AFM morphology of macroscopic PNIPAM-based hydrogels in their natural environment is challenging; in particular, the low modulus prevents stable imaging using standard
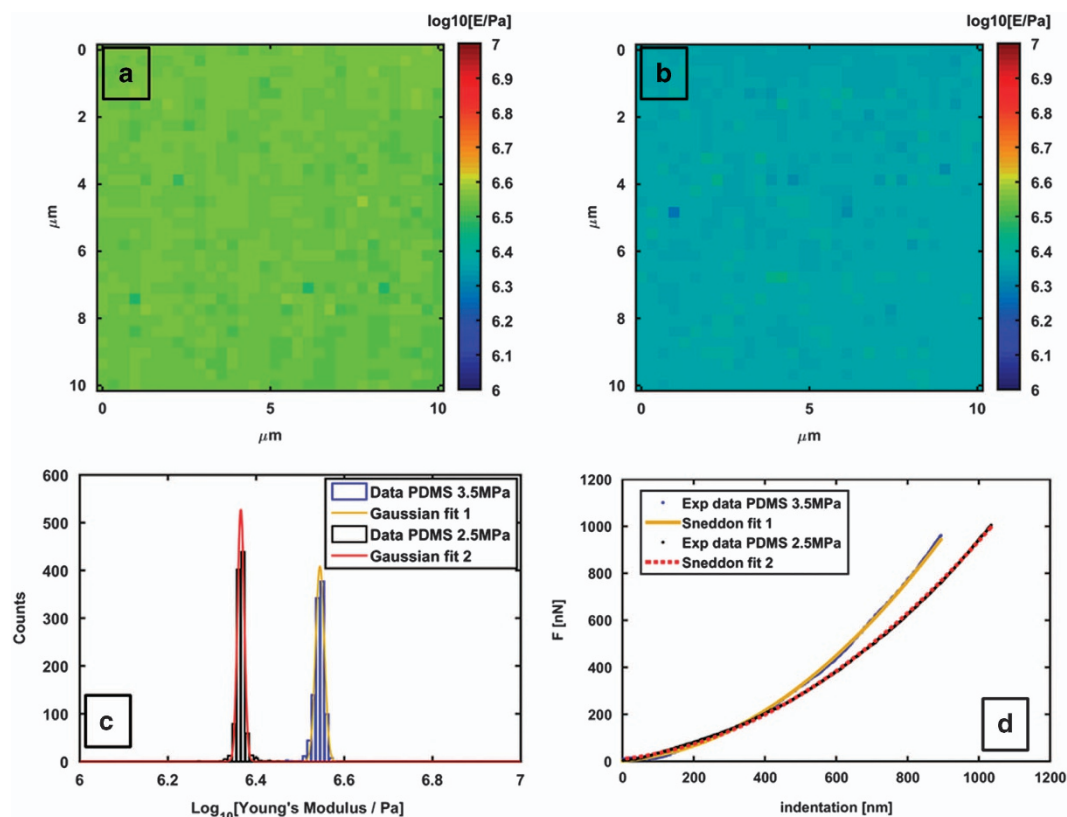

Figure 1 Mechanical Young's modulus map of PDMS (polydimethylsiloxane) calibration standards from Bruker; Young's modulus values are 3.5 and 2.5 MPa, respectively (**a**, **b**). Quantitative analysis of Young's modulus using Gaussian fit on log-normally distributed histograms (**c**). Examples of force vs indentation curves for the samples showing the raw data and fitting by the Sneddon model (**d**).
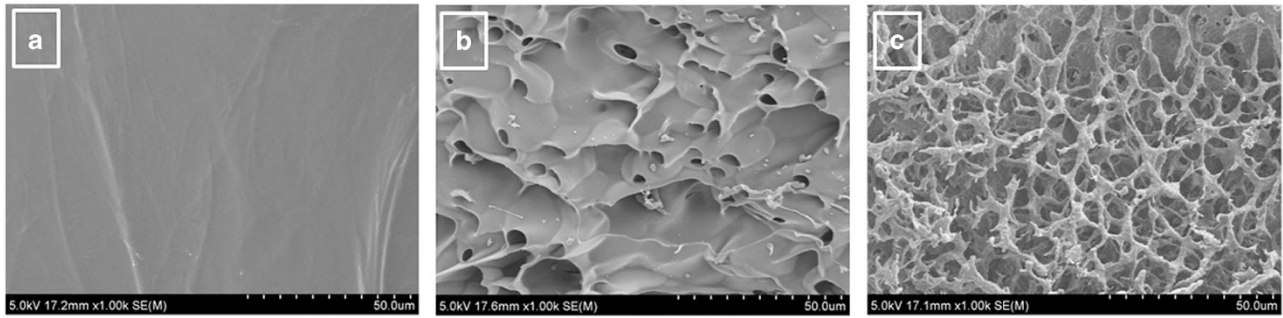
Figure 2 Surface morphology of the gels synthesized in (**a**) water (hydrogel-1), (**b**) 1:3 water–methanol (v v^{-1}) mixtures (hydrogel-2) and (**c**) 1:1 water–methanol (v v^{-1}) mixture (hydrogel-3).
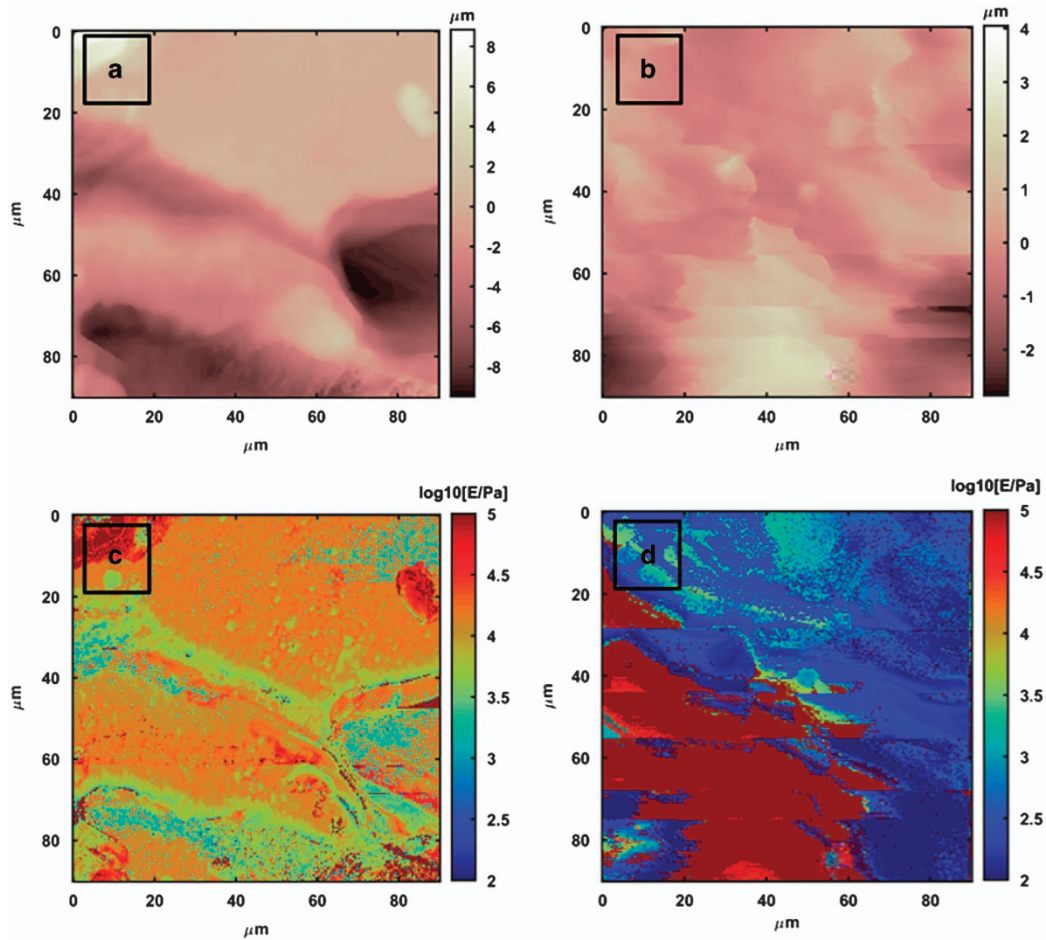

Figure 3 High-resolution force volume (FV) (256×256) compressed morphology (**a**) and Young's modulus mechanical map (**c**) for hydrogel-1. Same order of images for hydrogel-2 (**b**, **d**).

techniques (contact mode, tapping mode and PeakForce tapping). Examples of the morphology and high-resolution FV measurements (256×256) with a 90 μm scan size are presented for standard PNIPAM (hydrogel-1, morphology: Figure 3a, mechanical map: Figure 3c) and modified PNIPAM (hydrogel-2, morphology: Figure 3b, mechanical map: Figure 3d). The colloidal tip, used as the imaging probe, showed negligible convolution effects within the selected scan size. During imaging, FCs were captured at low resolution (256 points) and at high frequency (17 Hz), which resulted in an increase in noise and a poor

estimation of the Young's modulus (especially for the softest sample; Figure 3d). High-speed FC measurements in water, especially using soft cantilevers, are affected by dragging forces, which harm the contact point identification and final quantitative results (the same problem is encountered for PeakForce quantitative nanomechanical mapping).[22] Obtaining the high-resolution FV morphology for hydrogel-3 was not possible for the same reason. Morphologies in Figure 3 were not corrected using indentation because the poor contact point estimation results in an incorrect morphology.
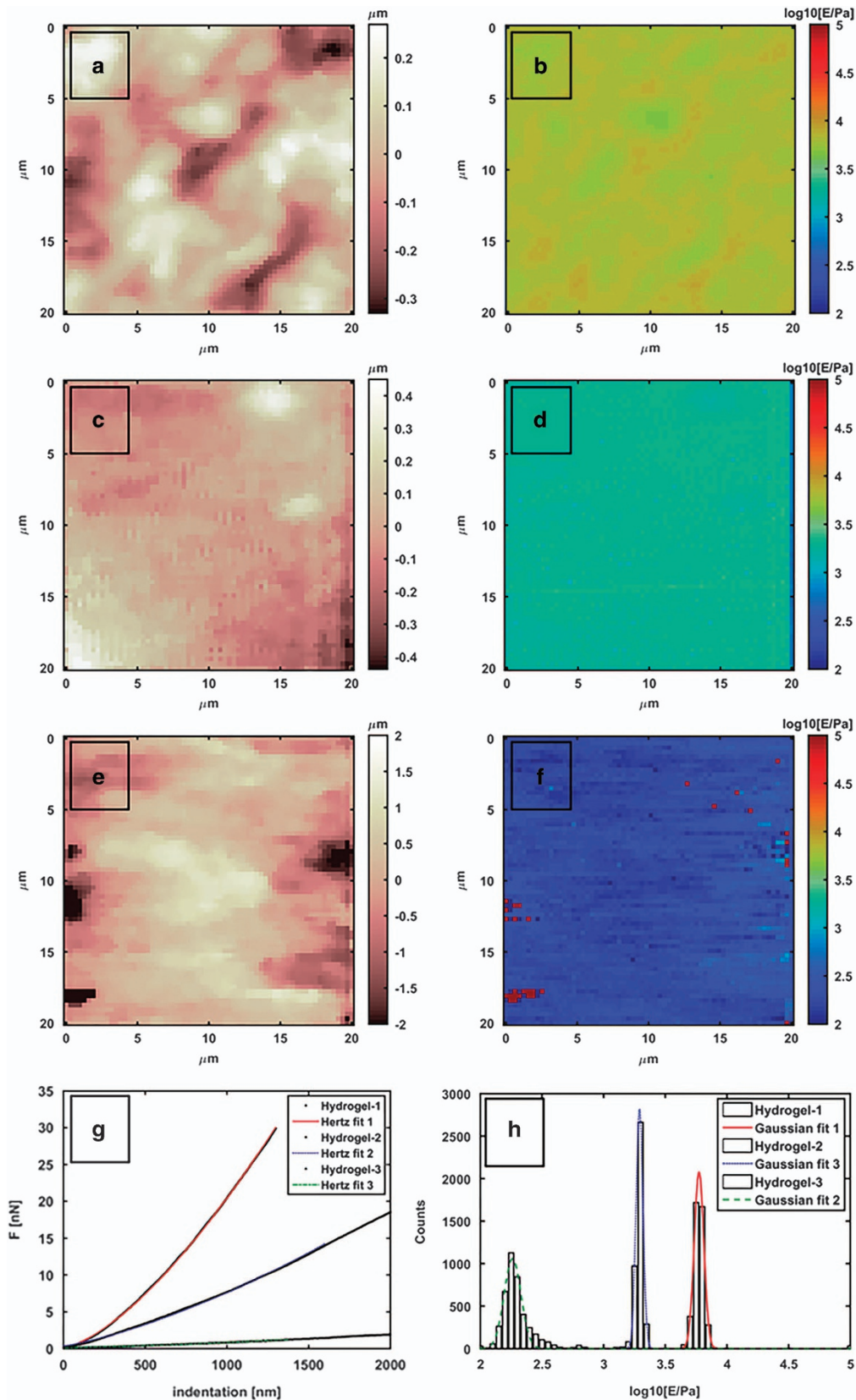
Figure 4 Medium-resolution force volume (FV) (64×64) morphology using 2550 nm radius colloidal tip (**a**) and Young's modulus mechanical map (**b**) for hydrogel-1. Same order of images for hydrogel-2 (**c**, **d**) and hydrogel-3 (**e**, **f**). (**g**) Force (nN) vs indentation (nm) graph of the three samples highlighting the raw data and Hertz fit. (**h**) Quantitative analysis using histograms of Young's modulus values in log-normal scale with a Gaussian distribution fit.

6

Moreover, the AFM images in water, presented in Figure 3, can be compared with SEM images on the same freeze-dried samples (Figure 2). The SEM morphology shows a surface with a plain, compact and defect-free structure for hydrogel-1 and an increased porosity for hydrogel-2. The AFM image is in agreement with the SEM results; by masking the macroscopically rough regions and focusing on the flat region in the upper part of hydrogel-1 (Figure 3a), the root mean square roughness is 200 nm, whereas the root mean square roughness for hydrogel-2 (Figure 3b) is 800 nm. Although the mechanical analysis is only qualitative because of low resolution in the FCs, there is a clear decrease in the Young's modulus value.

Mechanical analyses on the series of hydrogels were performed with lower resolution during imaging (64×64 or 16×16) but higher resolution in the FC measurements (4096 points and 3 Hz frequency), which allows for a much clearer, quantitative result. The mechanical properties of these gels are frequency-independent in the analysis range; therefore, the Young's modulus is unaffected by the tip approach speed (see Supplementary Figure 3 in SI.6 for experimental evidence on the measurement frequency). Raw data FCs were analyzed, as described in Materials and methods (Data analysis), with a particular focus on ensuring that the data obtained by colloidal tips did not exceed the Hertz model limitation ($\delta/R \ll 1$). Figure 4 represents typical data analysis output for three different samples measured in liquid using a colloidal tip with a radius of 2550 nm: hydrogel-1 (Figure 4a, morphology; Figure 4b, mechanical map), hydrogel-2 (Figure 4c, morphology; Figure 4d, mechanical map) and hydrogel-3 (Figure 4e, morphology; Figure 4f, mechanical map).

For high-resolution morphologies, modifying the solvents during synthesis leads to a clear modification in the mechanical response. The samples show an increased porosity, which is reflected by a less compact and ordered structure; therefore, a lower force is required to indent the sample surface (Figure 4g), which leads to a decrease in the Young's modulus distribution values (Figure 4h). The broader distribution in Figure 4h for hydrogel-3 is a concomitant effect of a logarithmic scale and an augmented porosity; these cause an increase in the relative error.

Figure 5 shows all the averaged Young's modulus data for three different types of gels measured with colloidal and sharp probes, and compared with the rheometer results (the numerical values presented in Supplementary Table 2). The shear modulus from the rheological measurements at 23 °C was converted into the Young's modulus for direct comparison using the Trouton ratio.[23] The Young's moduli

from both AFM and rheometer show a decreasing trend from hydrogel-1 to hydrogel-3, which is in agreement with the observed porosity and irregularity.[12] The sharp tip shows good qualitative results but a general overestimation of the absolute values. This behavior could be attributed to a poor calibration of the probe geometry and an intrinsic tendency for modulus overestimation in soft samples.[13,24] This tendency is mostly attributed to the underestimation of the contact area between tip and sample[10] and the nonlinearity of the elastic response when high local pressures are involved during the indentation process.[13]

The results from colloidal tips are more quantitative in terms of their absolute values, but they show inaccuracy for supersoft samples near 100 Pa. For such soft samples, a small applied force produces an indentation in the micrometer range (see hydrogel-3 in Figure 4g) and the validity of the Hertz model is compromised.[8,13] Decreasing the maximum force applied to diminish the indentation leads to a reduction in the signal-to-noise ratio and additional inaccuracy in contact point evaluation. For samples of ~ 100 Pa, mechanical measurements using AFM are still possible but the quantitative mechanical analysis is limited by the model used or experimental inaccuracy.

Mechanical analysis on the hydrogel-1 composite filled with Al_2O_3 nanoaggregates was performed using pyramidal tips (semiangle aperture $\theta = 19°$) in the FV mode. Hydrogel-1, without the embedded nanoaggregates, shows a Young's modulus of 6800 Pa for the spherical probe and 16 000 Pa for the sharp probe, as shown in Figure 5. Sharp probes were preferred to achieve sufficient spatial resolution to clearly distinguish the nanoaggregates. The maximum force applied during the measurements was ~ 80 nN, which resulted in an average indentation of 1500 nm. As shown in the morphology maps in Figure 6, the compressed morphology map (Figure 6a) must be corrected using indentation values to obtain a real morphology map at zero force (Figure 6b). Using the same force applied during the FV measurements, the indentation values will be different because of the heterogeneous Young's moduli, which lead to heavy distortions in the compressed morphology. Interestingly, the SEM analysis (Figure 6d) shows deviations from the morphology of the standard hydrogel-1 (Figure 2a). The increased roughness and irregularity can be attributed to the formation of defects in the hydrogel matrix because of the non-ideal interaction between the crosslinker and polymer chains. Nanoaggregates on top of the surface are visible in the AFM and SEM images (highlighted with red circles in Figure 6d). A detailed analysis of these systems, by varying the concentration and the size of filler, is in progress and will be presented in future work.

Mechanical properties were obtained using 25% of the total indentation range, and the maximum indentation was obtained with a maximum applied force (80 nN). The indentation range was decreased to minimize lateral shifts of the hard aggregates in the soft gel matrix during the indentation process. Lateral shifts produce a sudden change in the slope of the indentation curve, and they are easily recognizable, especially when the tip indentation is near the borders of particles. As expected from soft matrices filled with hard particles, the averaged mechanical properties of the surface are modified.[14,15,25] The averaged Young's modulus of hydrogel-1 using the sharp probe is 16 kPa, whereas for hydrogel-1 filled with 5% of Al_2O_3 nanoaggregates, the averaged Young's modulus increases up to 52 kPa (the numerical values are presented in Supplementary Table 2). Nanoaggregates on top of the surface appear inhomogeneous and harder (in some points, the Young's modulus value exceeds 500 kPa) than the background matrix, as shown in Figure 6c. By keeping the maximum force constant during FV measurements,
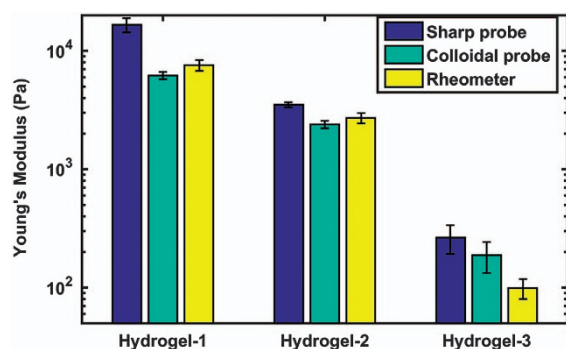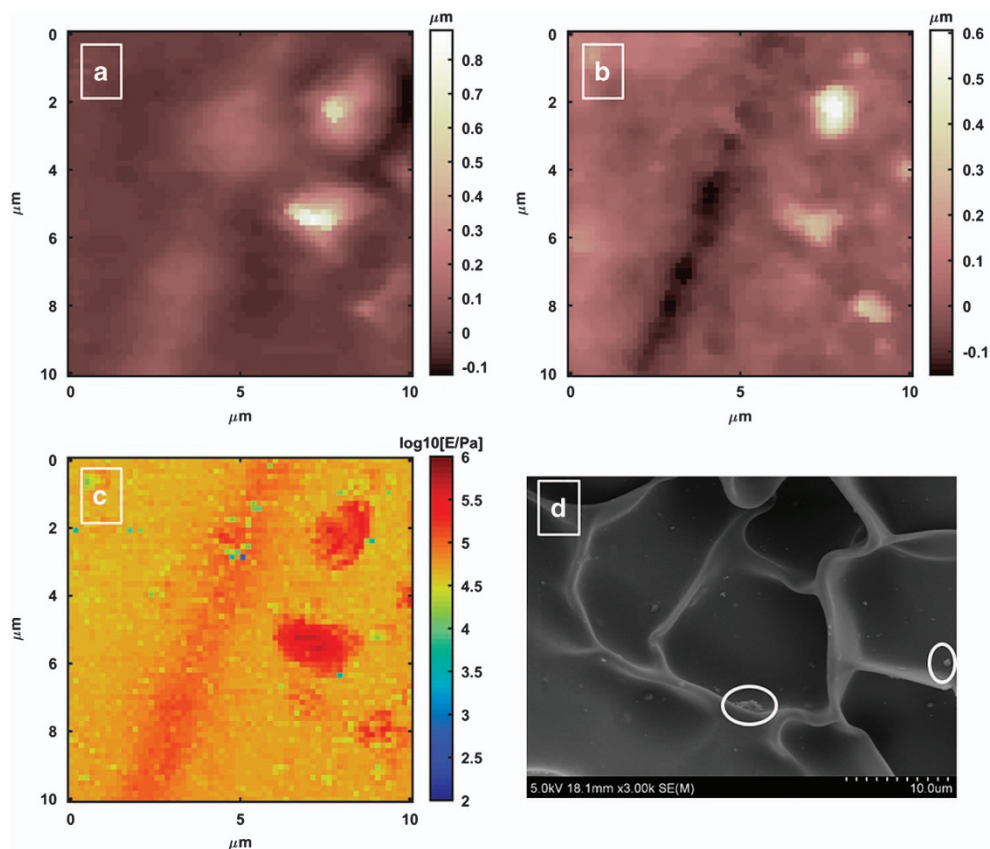

Figure 5 Young's modulus values for poly(N-isopropylacrylamide) (PNIPAM) hydrogels synthesized in different solvent compositions (hydrogel-1, -2 and -3). Atomic force microscopy (AFM) results obtained with sharp pyramidal tips and spherical colloidal tips are compared with values obtained from rheometer shear modulus results.

Figure 6 Medium-resolution force volume (FV) (64×64) compressed morphology (**a**) and corrected morphology (**b**), using sharp pyramidal probe, for hydrogel-1 filled with Al_2O_3 nanoaggregates in 5% weight concentration. Young's modulus map (**c**) using 20 nN indentation force in 1:1 correspondence with the morphology. Scanning electron microscopy (SEM) imaging of the same freeze-dried sample (**d**). White circles show nanoparticle aggregates inside hydrogel surface.

Table 1 Optimized parameters used in force volume measurements

K (N m^{-1})	Tip radius (spherical)	Tip semiangle (sharp)	Lateral size (µm)	Resolution	Scan rate (Hz)
0.07	2550	17	20×20	64×64	0.07
v_{appr} (µm s^{-1})	v_{ret} (µm s^{-1})	Ramp rate (Hz)	FC length (µm)	FC points	Force trigger (nN)
27–45	500–830	4.34	6–10	4096	20–5
Total time of measurement (min)	15				

Cells with double values represent 'hard' hydrogel-1 and 'soft' hydrogel-3 (softer). All parameters are explained in the Materials and methods section.

when the probe is indented on top of the nanoaggregates, the local pressure transferred to the underlying gel matrix is lowered. This reduction in the applied pressure is due to the increase of the contact area between nanoaggregates (used here as the effective indenter) and the hydrogel matrix.

CONCLUSIONS

We have demonstrated the capability of AFM for measuring the local mechanical properties of soft and ultrasoft hydrogels using the force spectroscopy technique combined with imaging. Table 1 lists the optimized parameters used in the FV measurements. The quantitative performance and reliability are mainly dependent on the probe geometry and, consequently, on the chosen model. Therefore, a comparison with macroscopic rheological measurements was necessary. Spherical colloidal probes demonstrated a superior performance in the quantitative characterization and showed good agreement with rheological data. This is mainly due to the defined geometry of the probe, better mechanical stability and reduced local pressure. Colloidal probes represent the best choice for obtaining mechanical properties with micrometric spatial resolution. Although standard pyramidal probes showed an overestimation of the Young's moduli, the measured trend is qualitatively in agreement with the results from colloidal probes and rheometer measurements, which represents a means for achieving nanometric spatial resolution. Both AFM probes showed deviations for samples with Young's moduli below 100 Pa. The nonconsistency of the model for high indentation or the poor

force resolution at low indentation prevents its application for quantitative analysis; on the other hand, this is easily achieved by using a rheometer. This study represents the first attempt to quantitatively validate AFM not only in the MPa Young's modulus range but also for very soft materials (0.1–10 kPa). The successful validation performed by rheology will be the starting point for mechanical characterization of more complex heterogeneous systems such as soft composite materials and soft biomaterials (living cell and tissues). In addition, the advantage of using AFM for obtaining local nanomechanical properties was shown on a heterogeneous sample: a hydrogel nanocomposite consisting filled with hard nanoparticle aggregates. By using a sharp probe to achieve a submicrometric spatial resolution, hard aggregate particles were shown to be harder than the surrounding hydrogel matrix. Further studies are being conducted on the use of geometrically well-defined fillers with different size distributions.

CONFLICT OF INTEREST

The authors declare no conflict of interest.

ACKNOWLEDGEMENTS

1 Butt, H.-J., Cappella, B. & Kappl, M. Force measurements with the atomic force microscope: technique, interpretation and applications. *Surf. Sci. Rep.* **59**, 1–152 (2005).

2 Radmacher, M., Tillmann, R. W. & Gaub, H. E. Imaging viscoelasticity by force modulation with the atomic force microscope. *Biophys. J.* **64**, 735–742 (1997).

3 Alessandrini, A. & Facci, P. AFM: a versatile tool in biophysics. *Measure. Sci. Technol.* **16**, R65 (2005).

4 Kasas, S. & Dietler, G. Probing nanomechanical properties from biomolecules to living cells. *Pflügers Archiv.* **456**, 13–27 (2008).

5 Alcaraz, J., Buscemi, L., Grabulosa, M., Trepat, X., Fabry, B., Farré, R. & Navajas, D. Microrheology of human lung epithelial cells measured by atomic force microscopy. *Biophys. J.* **84**, 2071–2079 (2003).

6 Rotsch, C. & Radmacher, M. Drug-induced changes of cytoskeletal structure and mechanics in fibroblasts: an atomic force microscopy study. *Biophys. J.* **78**, 520–535 (2000).

7 Mahaffy, R. E., Park, S., Gerde, E., Käs, J. & Shih, C. K. Quantitative analysis of the viscoelastic properties of thin regions of fibroblasts using atomic force microscopy. *Biophys. J.* **86**, 1777–1793 (2004).

8 Puricelli, L., Galluzzi, M., Schulte, C., Podesta, A. & Milani, P. Nanomechanical and topographical imaging of living cells by atomic force microscopy with colloidal probes. *Rev. Sci. Instrum.* **86**, 033705 (2015).

9 Liu, F. & Tschumperlin, D. J. Micro-mechanical characterization of lung tissue using atomic force microscopy. *J. Vis. Exp.* **54**, e2911 (2011).

10 Harris, A. R. & Charras, G. T. Experimental validation of atomic force microscopy-based cell elasticity measurements. *Nanotechnology* **22**, 345102 (2011).

11 Biswas, C. S., Patel, V. K., Vishwakarma, N. K., Mishra, A. K., Bhimireddi, R., Rai, R. & Ray, B. Synthesis, characterization, and drug release properties of poly (*N*-isopropylacrylamide) gels prepared in methanol–water cononsolvent medium. *J. Appl. Polym. Sci.* **125**, 2000–2009 (2012).

12 Biswas, C. S., Vishwakarma, N. K., Patel, V. K., Mishra, A. K., Saha, S. & Ray, B. Synthesis and study of the properties of stereocontrolled poly(*N*-isopropylacrylamide) gel and its linear homopolymer prepared in the presence of a Y(OTf)(3) Lewis acid: effect of the composition of methanol–water mixtures as synthesis media. *Langmuir* **28**, 7014–7022 (2012).

13 Dimitriadis, E. K., Horkay, F., Maresca, J., Kachar, B. & Chadwick, R. S. Determination of elastic moduli of thin layers of soft material using the atomic force microscope. *Biophys. J.* **82**, 2798–2810 (2002).

14 Haraguchi, K. Nanocomposite hydrogels. *Curr. Opin. Solid State Mater. Sci.* **11**, 47–54 (2007).

15 Peak, C. W., Wilker, J. J. & Schmidt, G. A review on tough and sticky hydrogels. *Colloid Polym. Sci.* **291**, 2031–2047 (2013).

16 Butt, H. J. & Jaschke, M. Calculation of thermal noise in atomic force microscopy. *Nanotechnology* **6**, 1 (1995).

17 Schulte, C., Ferraris, G. M. S., Oldani, A., Galluzzi, M., Podestà, A., Puricelli, L., de Lorenzi, V., Lenardi, C., Milani, P. & Sidenius, N. Lamellipodial tension, not integrin/ligand binding, is the crucial factor to realise integrin activation and cell migration. *Eur. J. Cell Biol.* **95**, 1–14 (2016).

18 Schulte, C., Rodighiero, S., Cappelluti, M. A., Puricelli, L., Maffioli, E., Borghi, F., Negri, A., Sogne, E., Galluzzi, M., Piazzoni, C., Tamplenizza, M., Podestà, A., Tedeschi, G., Lenardi, C. & Milani, P. Conversion of nanoscale topographical information of cluster-assembled zirconia surfaces into mechanotransductive events promotes neuronal differentiation. *J. Nanobiotechnol.* **14**, 1–24 (2016).

19 Sneddon, I. N. The relation between load and penetration in the axisymmetric boussinesq problem for a punch of arbitrary profile. *Int. J. Eng. Sci.* **3**, 47–57 (1965).

20 Bilodeau, G. G. Regular pyramid punch problem. *J. Appl. Mech.* **59**, 519–523 (1992).

21 Lybanon, M. A better least-squares method when both variables have uncertainties. *Am. J. Phys.* **52**, 22–26 (1984).

22 Minary-Jolandan, M. & Yu, M.-F. Nanomechanical imaging of soft samples in liquid using atomic force microscopy. *J. Appl. Phys.* **114**, 134313 (2013).

23 Trouton, F. T. On the coefficient of viscous traction and its relation to that of viscosity. *Proc. R. Soc. Lond A* **77**, 426–440 (1906).

24 Costa, K. D. & Yin, F. C. P. Analysis of indentation: implications for measuring mechanical properties with atomic force microscopy. *J. Biomech. Eng.* **121**, 462–471 (1999).

25 Schexnailder, P. & Schmidt, G. Nanocomposite polymer hydrogels. *Colloid Polym. Sci.* **287**, 1–11 (2008).

Supplementary Information accompanies the paper on the NPG Asia Materials website (http://www.nature.com/am)